Journal of Science and Technology – Smart Systems and Devices
Volume 36, Issue 3, September 2026, 027-037

An Integrated GIS Framework for Equitable Rooftop Solar Deployment and Distribution Grid Prioritization

Atharva Gujarathi[1], Sahil Manikshete[1], Vikram Velankar[1], Prasidh Shetty[1], Hai Bui Van[2,*]

[1]Department of Computer and Information Science, University of Michigan-Dearborn, MI, USA
[2]Department of Electrical and Computer Engineering, University of Michigan-Dearborn, MI, USA
[*]Corresponding author email: vhbui@umich.edu

Abstract

Distribution system planning increasingly requires integrated approaches that connect building-level renewable energy potential, household affordability, and grid infrastructure priorities within a unified and reproducible framework. However, rooftop solar suitability studies typically focus only on technical potential, energy equity assessments rarely inform grid planning, and grid asset prioritization often relies primarily on connected customer counts. This paper proposes a two-stage geographic information system (GIS) framework that integrates rooftop solar suitability, socioeconomic affordability, and distribution grid prioritization. In Stage 1, eligible buildings are evaluated using a technical suitability score incorporating regional solar resources, usable rooftop area, and the ratio of modeled photovoltaic (PV) generation to electricity demand. Neighborhood-level affordability indicators derived from the American Community Survey are then used to determine appropriate solar deployment pathways rather than excluding economically constrained households. In Stage 2, PV generation is incorporated into building-level residual demand, which is spatially aggregated to candidate substations, identified through geographic proximity rather than verified feeder connectivity, to reassess their relative planning priorities. The framework is demonstrated using five U.S. Census ZIP Code Tabulation Areas in southeastern Michigan. After data deduplication and boundary validation, 63,187 unique building records were identified, of which 22,445 met the required building classification, footprint, and socioeconomic data criteria. Under the base scenario, 1,891 buildings were assigned a green energy pathway, reducing modeled annual electricity demand from 1.031 TWh to 0.815 TWh, corresponding to a 20.93% reduction. Among 1,610 technically suitable residential buildings, 889 (55.2%) were directed toward community solar or financing-supported adoption based on neighborhood affordability. Incorporating distributed PV also altered grid planning priorities: 24 of 36 candidate substations changed rank and five changed priority class. Across sensitivity scenarios, modeled demand reductions ranged from 0.60% to 52.79%.

Keywords: Distributed energy resources, energy equity, geographic information systems, grid planning, solar photovoltaics.

1. Introduction

Electricity distribution systems are being reshaped by distributed energy resources (DERs), particularly rooftop PV systems and small-scale battery storage. Conventional distribution planning was developed under the assumption that demand at a given location grows predictably, and that the importance of a substation can be inferred from the number of connected customers or from historical peak load [1, 2]. When a nonuniform share of the buildings served by a location begins to generate part of its own energy, both assumptions weaken. The quantity relevant to planning is no longer gross demand but the demand remaining after local generation, and this residual quantity is not distributed across the network in the same manner as the original load [3].

The practical consequence is that two planning questions that are typically addressed separately become inherently interconnected. The first is which buildings are most suitable for distributed generation deployment, and the second is which grid locations remain critical after distributed generation is deployed. A framework that addresses the first question without incorporating its outcomes into the second can quantify distributed generation potential, but it cannot capture how the proposed deployment reshapes demand patterns and, consequently, grid planning priorities.

1.1. Related work and Research Gap

GIS-based methods are well established for estimating rooftop PV potential. National assessments combine LiDAR-derived roof planes with irradiance models to estimate technical potential at high spatial resolution [4], and city-scale studies couple the same geometry with hourly irradiance simulation [5, 6]. Where airborne survey data are unavailable, open footprint sources such as OpenStreetMap are viable inputs for regional studies, provided their heterogeneity in completeness and attribute quality is addressed explicitly [7]. These studies determine where PV could physically be installed, but generally do not address which households could realistically adopt it, nor do they propagate their results into network planning decisions.

p-ISSN 3093-3285
e-ISSN 3093-3315
https://doi.org/10.51316/jst.192.ssad.2026.36.3.4
Received: Aug 14, 2026; Revised: Sep 6, 2026;
Accepted: Sep 6, 2026; Online: Sep 14, 2026

A second body of work concerns energy equity. Energy justice research distinguishes distributional, procedural, and recognition dimensions of who benefits from an energy transition [8]. Empirical evidence from the U.S. solar market indicates that adoption is concentrated in higher-income and owner-occupied housing even after controlling for technical potential, and that supply-side factors such as income-targeted marketing reinforce it [9, 10]. Community solar and financing-supported programs exist specifically to reach households for which direct rooftop ownership is not realistic [11, 12]. This literature identifies the deployment mechanism, rather than the roof itself, as the binding constraint in many neighborhoods.

Combining the two naively creates a methodological problem. A framework that inserts an affordability term directly into a suitability score would rate a lower-income household as less suitable than an otherwise identical higher-income household with the same roof, orientation, and demand, thereby encoding the existing adoption gap as a technical conclusion.

The gap addressed in this paper is therefore the absence of a single reproducible workflow connecting three layers that are usually studied separately: technical rooftop suitability, socioeconomic deployment feasibility, and grid location prioritization. The specific research question is whether an equity-aware assignment of DER pathways at the building level produces a residual demand distribution that changes which substations are most important, and whether that change can be quantified using public data alone.

1.2. Contributions

The contributions of this paper are threefold.

1) A two-stage planning framework is formulated in which technical suitability and affordability are deliberately decoupled, so that affordability determines the deployment mechanism rather than excluding a building. Distinct decision logics based on equity, economics, and resilience are applied to the building categories for which each is appropriate.

2) Building-level outcomes are propagated quantitatively into a residual demand model aggregated at candidate substations. This renders the grid consequence of building-level decisions measurable and enables a demand-aware ranking to be compared directly against the conventional building-count heuristic.

3) The framework is demonstrated end to end on a reproducible public data pipeline covering 63,187 validated building records, with explicit separation of observed, derived, and assumed quantities, an automated validation suite, and scenario-based sensitivity analysis.

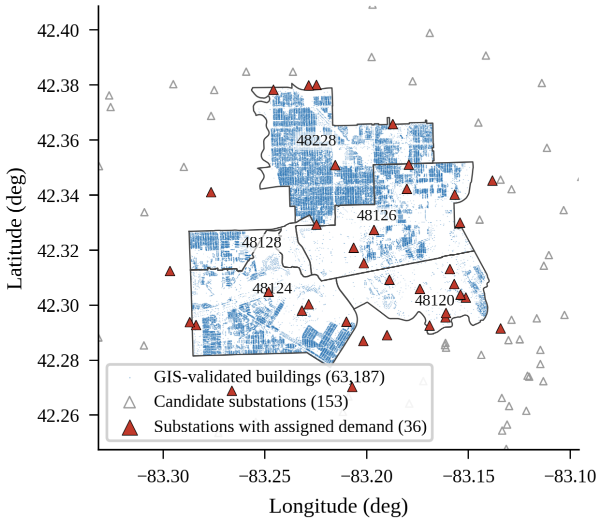

Fig. 1. GIS-validated study area, building records, and candidate substations

2. Study Area, Data, and Geographic Information Systems Integration

2.1. Study Area and Public Data Sources

The study area comprises five U.S. Census ZIP Code Tabulation Areas (ZCTAs) in Wayne County, Michigan: 48120, 48124, 48126, 48128, and 48228. The area combines dense residential blocks, a substantial industrial corridor, and neighborhoods with markedly different socioeconomic conditions within a compact geographic footprint, making it a suitable test case for equity-aware planning.

Four public sources are used. Building footprints and power facilities were retrieved from OpenStreetMap through the Overpass application programming interface [13]. Official area boundaries and block-group geometry were obtained from the 2025 Census TIGER/Line files [14]. Median household income, owner occupancy, and poverty estimates were obtained from the 2024 American Community Survey (ACS) five-year release [15]. Annual mean global horizontal irradiance (GHI) and 10 m wind speed were obtained from the NASA POWER climatology for 2015 to 2024 [16]. No proprietary utility data, metered consumption, or commercial imagery were used, so the pipeline can be reproduced by a third party at no cost. Fig. 1 shows the study area, the validated building records, and the candidate substations.

2.2. Geographic Information Systems Integration and Deduplication

The Overpass query was tiled across the study region, which produces repeated features wherever tiles overlap. Stable OpenStreetMap identifiers were therefore used as the deduplication key, and every retained feature was validated against the official ZCTA polygons by spatial intersection rather than by a rectangular search envelope. This procedure reduced an

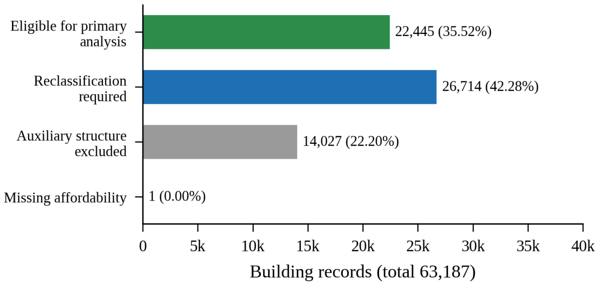

Fig. 2. Analysis eligibility of the 63,187 GIS-validated building records

initial extraction of more than 200,000 raw records to 63,187 unique and geographically validated buildings. Polygon geometry was preserved for every record, and footprint area was computed on an equal-area projection, yielding complete footprint coverage.

The five areas contribute 1,554 records in 48120, 15,422 in 48124, 10,455 in 48126, 4,447 in 48128, and 31,309 in 48228, so the spatial distribution of the dataset is strongly uneven.

2.3. Building Classification and Eligibility

Building tags were mapped to seven analysis categories, together with a generic class for features carrying only the tag `building=yes` and an unclassified class for the remaining cases. Three eligibility outcomes follow, summarized in Fig. 2.

Auxiliary structures such as garages, sheds, carports, roofs, and parking structures were excluded, because they do not represent independent electrical loads and treating them as separate buildings would inflate both the population and the modeled demand. This removed 14,027 records. Generic and unclassified features were flagged as requiring reclassification and withheld from the energy model while remaining in the master dataset, affecting 26,714 records. One residential record lacked usable socioeconomic data. The remaining 22,445 records form the primary analysis population, whose composition and associated base parameters are given in Table 1. The excluded records are retained in the published dataset rather than deleted, which keeps the filtering auditable and provides a clear target for future classification work.

2.4. Proximity-Based Substation Assignment

The facility extraction returned 167 public power features, of which 153 are tagged as substations and 14 as generating plants. Only substations are eligible for assignment, because generating plants are not distribution service points. Every validated building was assigned to the geographically nearest candidate substation using Haversine distance evaluated with a ball tree structure.

The resulting assignment is spatially compact, with a mean distance of 0.737 miles and a 95th percentile of 1.290 miles. Thirty six of the 153 candidate substations

Table 1. Primary analysis population and the base-scenario parameters applied to each building category

Category	**n**	f_c^{roof}	L_c	**EUI**	a_c^{min}	a_c^{tgt}
Residential	21,375	0.65	1.5	12	250	1,600
Commercial	769	0.75	1.5	18	1,000	8,000
Industrial	165	0.75	1.0	20	2,500	20,000
Religious	66	0.60	1.5	8	750	5,000
Hospital	54	0.65	3.0	35	1,500	12,000
School	11	0.70	2.0	12	1,500	12,000
Emergency	5	0.65	1.5	20	750	5,000
Total	**22,445**					

f_c^{roof} is the usable roof fraction and L_c the default floor count used when OpenStreetMap does not report building levels. EUI is the annual energy use intensity proxy in kWh/ft^2/yr. a_c^{min} and a_c^{tgt} are the lower and upper references of the roof area score in ft^2.

receive at least one primary-analysis building and therefore constitute the Stage 2 planning units. The assignment is a geographic planning approximation rather than an electrical connectivity model, because feeder topology, service territories, and switching configuration are not public.

3. Sequential Planning Methodology

3.1. Framework Overview

The framework proceeds in two stages, shown in Fig. 3. Stage 1 assigns a deployment pathway to each eligible building and converts that pathway into an annual grid offset. Stage 2 subtracts those offsets from modeled demand and aggregates the remainder at candidate substations in order to reprioritize them. The two stages are connected by a single quantity, the residual demand, which renders the grid consequence of a building-level equity decision explicit and measurable.

Because the framework combines measured geometry with scenario assumptions, Table 2 records the status of every quantity used. Quantities marked as modeled are planning estimates produced under stated assumptions and are not measurements.

3.2. Stage 1: Technical Suitability

Technical suitability combines three bounded scores. The sunlight score normalizes the annual mean GHI of the ZCTA reference point between a lower bound G_{lo} of 2.5 and an upper bound G_{hi} of 5.0 kWh/m^2/day,

$$S_i = \text{clip}\left[\frac{GHI_i - G_{lo}}{G_{hi} - G_{lo}}, 0, 1\right] \tag{1}$$

where clip bounds its argument to the stated interval. Usable roof area is the footprint area A_i^{fp} multiplied by a category-dependent roof use fraction f_c^{roof} and a scenario multiplier μ_{roof}, capped at the footprint itself,

$$A_i^{use} = \min\left(A_i^{fp} f_c^{roof} \mu_{roof},\, A_i^{fp}\right) \tag{2}$$

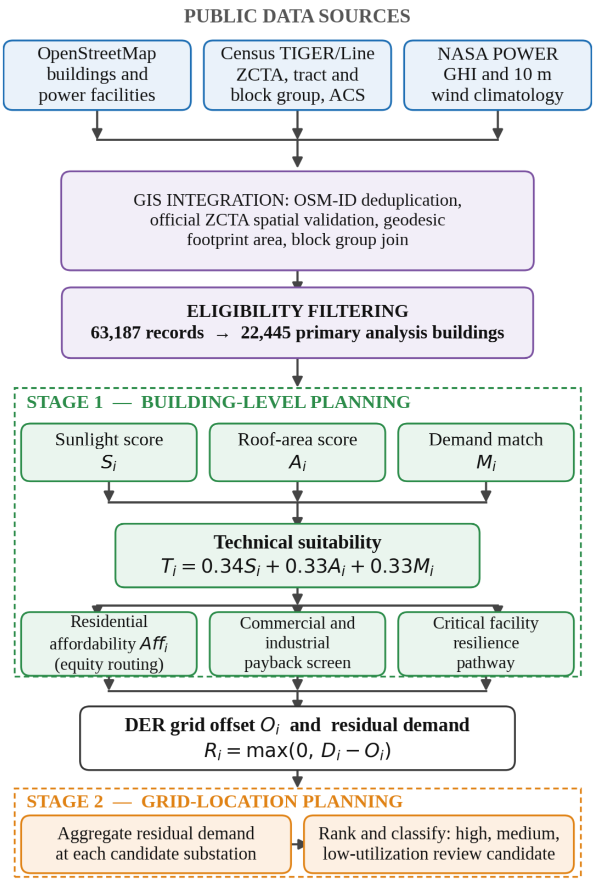

Fig. 3. The two-stage planning framework linking public data to grid location priorities

The fraction represents setbacks, mechanical equipment, roof geometry, maintenance access, and unfavorable orientation. It is an assumption, whereas the footprint it multiplies is observed geometry. The roof area score normalizes usable area between a category-specific lower reference a_c^{min} and target a_c^{tgt}, both listed in Table 1,

$$A_i = \text{clip}\left[\frac{A_i^{use} - a_c^{min}}{a_c^{tgt} - a_c^{min}}, 0, 1\right] \tag{3}$$

Annual electricity demand is modeled as floor area multiplied by a category-specific annual energy use intensity EUI_c, where floor area is the footprint multiplied by the observed number of levels L_i where reported and by the category default otherwise,

$$D_i = A_i^{fp} L_i EUI_c \mu_{EUI} \tag{4}$$

The intensity values are consistent in magnitude with the ranges reported by the national commercial and residential consumption surveys [17, 18], but are applied as uniform category proxies rather than building-specific measurements. PV capacity and annual generation follow from usable roof area, an assumed power density ρ of 0.015 kW/ft^2, the irradiance, and a performance ratio PR of 0.80 consistent with standard system loss

Table 2. Status of the quantities used in the framework

Quantity	**Status**	**Source or base value**
Building location	Observed	OpenStreetMap geometry
Footprint area	Derived	Equal-area projection
Building category	Derived	Rule-based mapping of tags
ZCTA, block group	Observed	2025 TIGER/Line join
Substation location	Observed	OpenStreetMap features
Assignment distance	Derived	Haversine nearest neighbor
Income, ownership	Observed	2024 ACS block group
Poverty rate	Observed	2024 ACS tract
Solar resource	Observed	NASA POWER 2015 to 2024
Usable roof fraction	Assumed	0.55 to 0.75 by category
Levels if absent	Assumed	1.0 to 3.0 by category
Energy use intensity	Assumed	8 to 35 kWh/ft^2/yr
PV power density	Assumed	0.015 kW/ft^2
Performance ratio	Assumed	0.80
Installed cost	Assumed	2,500 USD/kW
Electricity value	Assumed	0.16 USD/kWh
Grid offset share	Assumed	0.30 to 0.95 by pathway
Annual demand	Modeled	Floor area × EUI
PV generation	Modeled	Capacity, GHI, PR
Residual demand	Modeled	Demand minus offset
Substation priority	Output	Cumulative residual share

Observed quantities are taken directly from a public dataset. Derived quantities are computed from observed quantities without a behavioral assumption. Assumed quantities are scenario parameters and are varied in the sensitivity analysis.

assumptions [19],

$$P_i = A_i^{use} \rho \tag{5}$$

$$G_i = P_i \, GHI_i \times 365 \times PR \tag{6}$$

The generation to demand match is bounded at unity, so that oversizing a system beyond the demand of its own building does not further increase suitability,

$$M_i = \min(1, \; G_i / D_i) \tag{7}$$

The three components are combined with near-equal weights into a single technical suitability score bounded between zero and one,

$$T_i = 0.34\, S_i + 0.33\, A_i + 0.33\, M_i \tag{8}$$

A building is technically suitable in the base scenario when $T_i \geq 0.60$. The threshold for critical facilities is relaxed to 0.55, because their planning objective is resilience rather than energy yield.

The near-equal weighting of the three technical components follows common practice in GIS-based multi-criteria suitability assessment, where assigning equal weights to input criteria avoids introducing analyst-specific bias when no single criterion is established a priori as dominant [20]. The 0.34/0.33/0.33 split rather than an exact one-third each is a rounding convention with no material effect on the resulting score. The 0.60 threshold is set at a moderately high point on the 0 to 1 scale so that a building must combine adequate values across sunlight, roof area, and demand match rather than compensate a weak component with a strong one; because the sunlight score is fixed at 0.513 in this study area, meeting the threshold in practice requires roof area and demand match scores that are jointly well above their midpoints. The relaxed threshold of 0.55 for critical facilities reflects that their planning objective, service continuity during an outage, has value even at a lower level of technical suitability than is required to justify a purely economic rooftop investment. The higher threshold of 0.78 used for the residential solar-plus-battery pathway in Section 3.3 is set near the upper end of the observed suitability range so that battery pathways, which involve additional capital cost for on-site storage beyond the PV system itself, are reserved for buildings with the strongest technical case.

3.3. Equity-Aware Residential Deployment Pathways

Residential affordability is represented by a bounded neighborhood proxy constructed from three ACS variables: a robust normalization I_i of median household income, the owner-occupancy rate O_i, and the poverty rate V_i,

$$Aff_i = 0.50 I_i + 0.25\, O_i + 0.25\,(1 - V_i) \tag{9}$$

Half of the indicator is placed on income, which is most directly related to capital access, and the remainder is divided between tenure and poverty incidence. Tenure is included because a tenant cannot authorize a rooftop installation regardless of income.

Income and owner occupancy were obtained preferentially at block-group level with a tract-level fallback where an estimate is suppressed, and poverty at tract level. Of the 21,375 residential buildings, 19,053 use block-group income and 2,322 the tract fallback, with the geographic source recorded for every record and no random imputation. Coverage reaches 99.995%. The result is a neighborhood-level indicator and does not represent the income of the household occupying a specific building.

The central design decision is that affordability does not enter (8). If it did, two otherwise identical houses would receive different technical suitability scores because of neighborhood income. The recommendation is instead a function of technical suitability, affordability, and building category c_i,

$$Rec_i = f(T_i, Aff_i, c_i) \tag{10}$$

For a technically suitable residential building, an affordability value below $t_{low} = 0.45$ gives a community solar or incentive-support pathway; a value between 0.45 and $t_{high} = 0.65$ gives rooftop solar with financing or incentive support; a value at or above 0.65 gives a conventional rooftop solar pathway; and a value at or above 0.65 combined with $T_i \geq 0.78$ gives a solar-plus-battery pathway. A building failing the technical threshold is assigned continued grid dependence irrespective of affordability. Low affordability therefore never removes a building from the transition; it changes the mechanism by which the transition would be delivered.

The affordability thresholds of 0.45 and 0.65 were chosen to yield three subgroups of broadly comparable size within the observed distribution (8,800, 5,535, and 7,040 residential buildings, respectively) and are broadly consistent with the conventional low- and moderate-income banding used in U.S. housing policy, where households below 80% of area median income are designated low income and those below 50% are designated very low income for federal housing assistance eligibility [21]. Because the affordability index in this study blends income, tenure, and poverty into a single 0 to 1 proxy rather than a literal percentage of area median income, the two thresholds are best read as an application of that banding convention to a composite indicator rather than a direct translation of the federal percentages.

3.4. Nonresidential and Critical Facility Pathways

Household affordability is not meaningful for commercial, industrial, and religious buildings, so those categories are screened economically. Installed cost C_i is capacity multiplied by an assumed cost per kilowatt consistent with published system cost benchmarks [22], annual energy value is the locally usable generation multiplied by an assumed electricity value p, and the screen is a simple payback period,

$$\pi_i = \frac{C_i}{\min(G_i, D_i)\,p} \tag{11}$$

A nonresidential building becomes a commercial or industrial solar candidate when it satisfies both the technical threshold and a payback of no more than 15 years. Schools, hospitals, and emergency services are treated as critical facilities and receive a solar-plus-battery pathway when they satisfy the relaxed technical threshold, with a battery sized at four hours of average load. The framework thus applies three decision logics, based on equity, economics, and resilience, to the categories for which each is appropriate.

3.5. Residual Demand

Each pathway is associated with a grid offset share σ_r representing the proportion of local generation that displaces grid supply. In the base scenario the share is 0.80 for rooftop and financing-supported rooftop solar, 0.95 for both battery pathways, 0.85 for commercial and industrial solar, 0.30 of building demand for community solar participation, and zero for continued grid dependence. For all pathways other than community solar the offset applies to the locally usable generation,

$$O_i = \sigma_r \min(G_i, D_i) \tag{12}$$

whereas a community solar participant offsets a share of its own demand, since the generation is not located on its roof. The residual demand is then

$$R_i = \max(0,\, D_i - O_i) \tag{13}$$

which guarantees that baseline demand equals residual demand plus offset for every building.

3.6. Stage 2: Demand-Aware Substation Prioritization

For a candidate substation g with assigned building set $A(g)$, the baseline and residual demands are the corresponding sums,

$$D_g^{base} = \sum_{i \in A(g)} D_i, \qquad D_g^{res} = \sum_{i \in A(g)} R_i \tag{14}$$

Substations are ranked by descending residual demand and classified by cumulative share of the total,

$$\Phi_g = \frac{\sum_{h:\,\mathrm{rank}(h) \le \mathrm{rank}(g)} D_h^{res}}{\sum_h D_h^{res}} \tag{15}$$

Locations within the first 80% of cumulative residual demand are high priority, those between 80% and 95% are medium priority, and the remainder are low-utilization review candidates. The final class is a decision-support label: a low-utilization candidate carries a small share of modeled residual demand and may warrant engineering review, but this is not a recommendation to decommission, because feeder topology, capacity, protection coordination, and contingency performance are outside the scope of a public data framework.

3.7. Baselines, Validation, and Scenario Design

Two baselines are used. The first is a no-DER case in which every primary building remains grid dependent, which isolates the effect of Stage 1 on Stage 2 under otherwise identical assumptions. The second is a ranking by assigned building count, representing the conventional heuristic that the framework is intended to improve upon.

Every output passes an automated validation suite covering identifier uniqueness, boundary membership, substation-only assignment, bounded suitability scores, nonnegative residual demand, the energy balance identity of (13), and equality between building-level and facility-level totals. All 32 integrity checks and all seven paper-readiness checks pass in strict mode.

Because several parameters in Table 2 are assumptions rather than measurements, three scenarios vary them jointly. The conservative, base, and optimistic cases simultaneously change the roof use multiplier, the energy intensity multiplier, the technical threshold, both affordability thresholds, the solar offset multiplier, and the community solar participation share. As the parameters move together, the analysis measures sensitivity to a coherent set of planning assumptions and is correctly described as scenario-based rather than one factor at a time sensitivity.

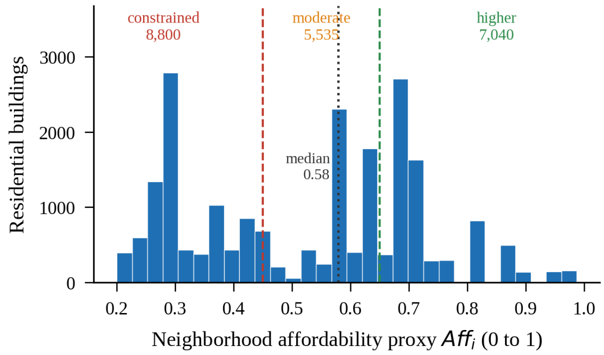

Fig. 4. Distribution of the neighborhood affordability proxy for the 21,375 residential buildings in the primary analysis population

4. Results and Discussion

4.1. Building-Level Suitability and Pathways

Fig. 4 shows the distribution of the affordability proxy. The distribution is multimodal, as expected because buildings within the same census geography share an estimate, and the median is 0.579. The three affordability groups contain 8,800 constrained, 5,535 moderate, and 7,040 higher-affordability residential buildings, so the equity layer is not concentrated in a single group.

Roof area is the dominant source of building to building variation in this study area. The sunlight score is constant at 0.513, because the irradiance product returns 3.7834 kWh/m^2/day for all five ZCTA reference points, and the demand match score has a standard deviation of only 0.026 across residential buildings, because only 1.2% of residential records report an observed number of levels. By comparison, the standard deviation of the roof area score is 0.200.

Under the base scenario, 1,891 of the 22,445 primary buildings receive a green energy pathway (8.43%) and 20,554 remain grid dependent. Table 3 and Fig. 5(a) give the distribution across the seven pathways, together with the modeled capacity and offset each contributes. The framework does not produce a binary solar or no solar answer; it distinguishes six qualitatively different deployment mechanisms.

4.2. The Equity Effect

Among residential buildings, 1,610 satisfy the base technical threshold. Their pathways are 692 conventional rooftop solar, 360 rooftop solar with financing or incentive support, 529 community solar or incentive support, and 29 solar-plus-battery. The 889 buildings in the second and third groups represent 55.2% of the technically suitable residential population, as shown in Fig. 5(b).

This is the central equity result. More than half of the homes physically capable of hosting a viable rooftop system are located in neighborhoods where direct ownership is not the realistic deployment mechanism. A framework embedding affordability inside the suitability

Table 3. Base-scenario planning pathways, modeled capacity, and contribution to the grid offset

Pathway	n	MW	GWh	%
Rooftop solar	692	23.5	20.7	9.6
Rooftop solar with financing	360	12.2	10.8	5.0
Community solar or incentive	529	24.6	13.8	6.4
Residential solar plus battery	29	1.1	1.1	0.5
Commercial or industrial solar	273	177.4	166.6	77.2
Critical facility solar, battery	8	2.6	2.7	1.3
All green pathways	**1,891**	**241.4**	**215.8**	**100.0**
Continued grid dependence	20,554	0.0	0.0	0.0

MW is modeled installed PV capacity, GWh the modeled annual grid offset, and the final column the share of the total modeled offset. Community solar capacity is reported at the participating building for comparability, although the physical array would be sited elsewhere.

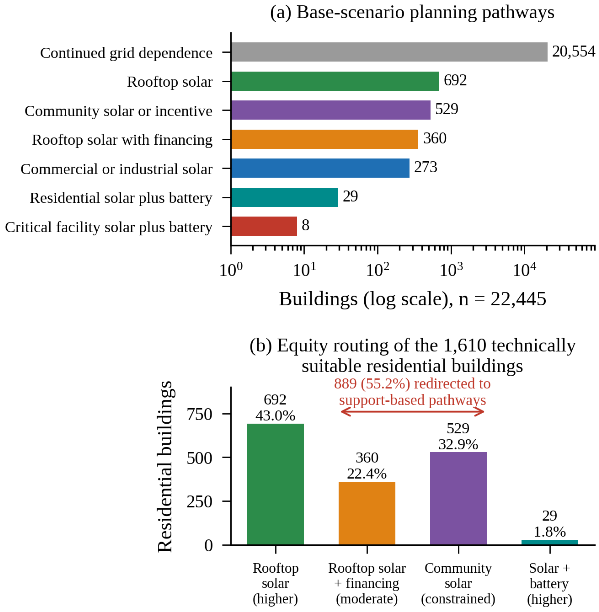

Fig. 5. (a) Base-scenario planning pathways. (b) Deployment pathways of the technically suitable residential buildings

score would have reported these buildings as less suitable and would have understated technical potential precisely in the neighborhoods that program design is intended to reach. By decoupling the two, the framework converts an affordability constraint into a concrete program requirement: community solar capacity or financing support for a specific and spatially located set of buildings.

Fig. 6 shows where those buildings are located. The community solar pathway clusters spatially and does not coincide with the conventional rooftop pathway, which is operationally relevant because a community solar program has its own siting and subscription geography.

4.3. Residual Grid Demand and Its Sources

The no-DER baseline for the primary population is 1.031 TWh/yr. Applying the base-scenario pathways and offset shares gives a residual demand of 0.815 TWh/yr and a total offset of 215.8 GWh/yr, so the modeled

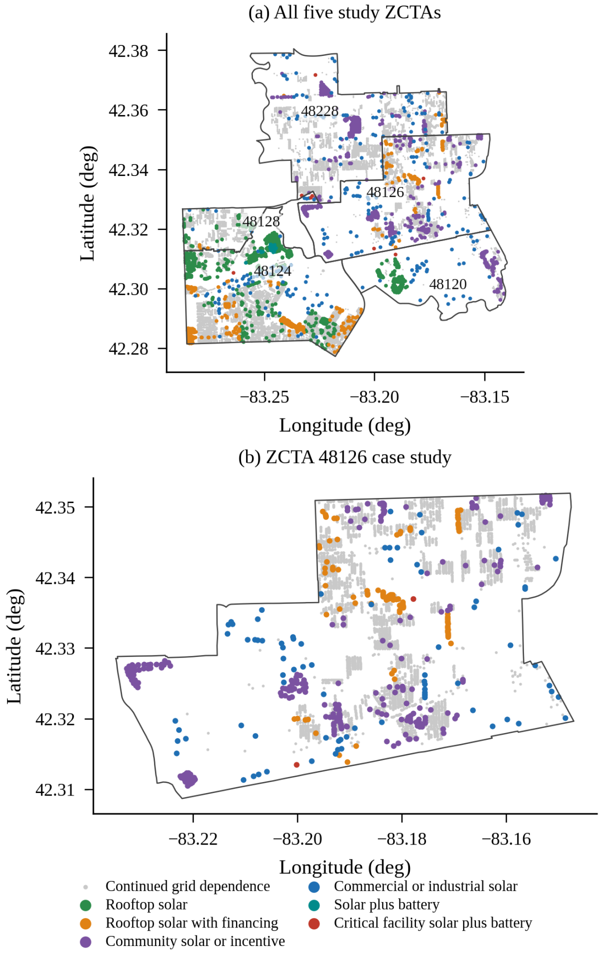

Fig. 6. Spatial distribution of the base-scenario pathways for (a) all five ZCTAs and (b) the 48126 case study

annual grid demand reduction is 20.93%. Fig. 7(a) shows the baseline and residual demand of the 18 largest candidate substations and indicates that the reduction is far from uniform, ranging from approximately 9% at one location to 49% at another.

Fig. 7(b) explains this asymmetry. Residential buildings constitute 95.2% of the primary population but contribute only 21.5% of the modeled offset, whereas commercial and industrial buildings constitute 4.2% of the population and together contribute 74.1%. A small number of large facilities combine extensive usable roof area with high energy use intensity, so a single commercial or industrial candidate can offset as much as several hundred houses. This provides the quantitative justification for Stage 2: if building count were an adequate proxy for grid importance, a category holding 4.2% of the buildings could not deliver three quarters of the effect.

The 54 hospital and medical buildings contribute no offset, because none reaches the relaxed critical facility threshold once the default of three levels raises their modeled demand while their footprints remain modest. This identifies medical facilities as the category most sensitive to improved height attribution.

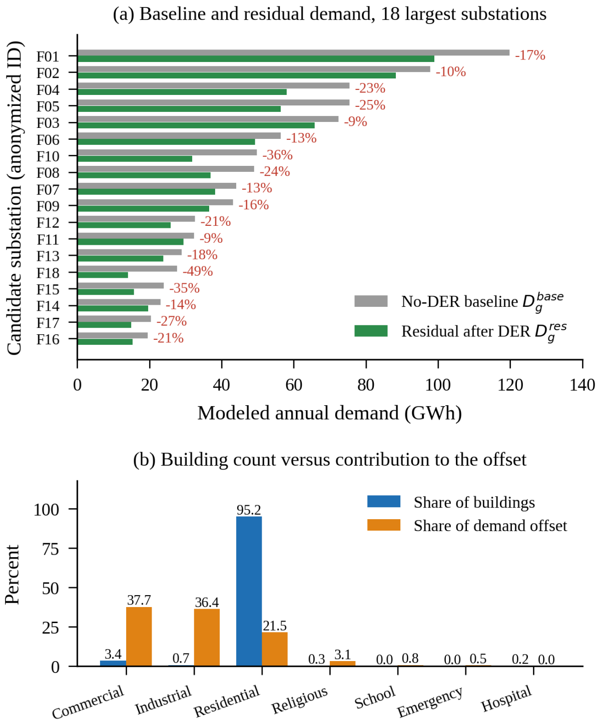

Fig. 7. (a) Baseline and residual demand of the largest candidate substations. (b) Building share against offset share by category.

Table 4. Candidate substations that change priority class after distributed adoption in the base scenario.

ID	Bldg	Base	Res	Red	From	To
F14	936	23.0	19.7	14.5	Medium	High
F15	303	24.0	15.7	34.6	High	Medium
F18	63	27.7	14.0	49.4	High	Medium
F22	526	10.5	9.9	5.3	Low util.	Medium
F25	3	16.5	7.8	52.8	Medium	Low util.

Base and Res are modeled baseline and residual annual demand in GWh, and Red the modeled percentage reduction. Identifiers are anonymized and assigned by residual demand rank; no utility-specific facility name or operator is used.

4.4. Substation Reprioritization

Thirty six candidate substations receive modeled demand. After the base-scenario offsets are applied, 24 of the 36 change rank, with a maximum change of five positions, and five change priority class. Table 4 lists the five reclassified locations.

The number of low-utilization review candidates is 12 both before and after distributed adoption. This is an important negative result: the framework does not reduce the number of grid locations required, but changes which locations are most critical.

The individual cases are informative. F18 serves only 63 buildings but carries a large baseline demand, and a 49.4% modeled reduction moves it from high to medium priority. F22 moves in the opposite direction, achieving only a 5.3% reduction, so as neighboring locations shed load it rises from a low-utilization candidate to medium priority. Neither movement would be detected by a ranking based on gross demand or building count.

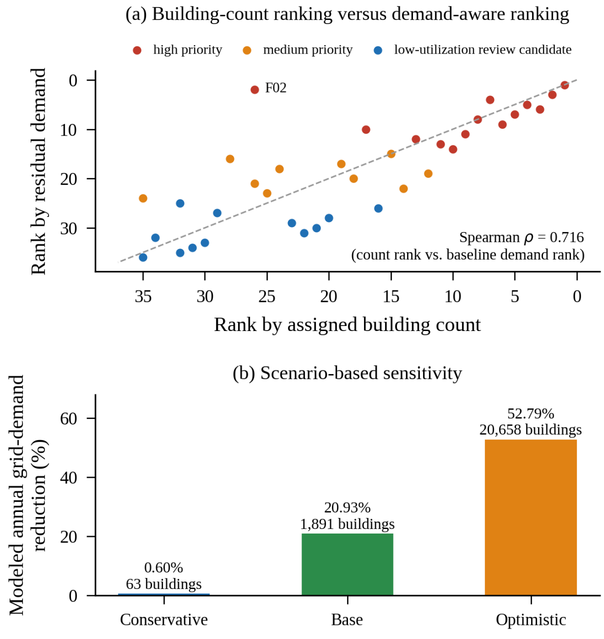

Fig. 8. (a) Building-count ranking against demand-aware ranking. (b) Modeled demand reduction under the three scenarios.

Fig. 8(a) compares the building-count ranking with the demand-aware ranking. The Spearman rank correlation between building-count rank and baseline demand rank is 0.716, and between building-count rank and residual demand rank it is 0.791. The relationship is positive but far from an identity. The clearest counterexample is F02, which serves only 49 buildings yet ranks second by demand in both the baseline and residual orderings. Counting connected buildings is therefore not equivalent to evaluating modeled energy demand.

4.5. Geographic Heterogeneity and the 48126 Case Study

Table 5 reports the results by ZCTA. Modeled reductions range from 10.04% in 48128 to 45.40% in 48120, and the ordering does not follow the number of buildings. ZCTA 48120 contains only 1,554 records and 608 primary buildings, yet achieves the largest reduction, because its primary population contains a high proportion of large industrial and commercial structures. ZCTA 48228 contains 31,309 records, roughly half of the dataset, but achieves 15.66%.

ZCTA 48126 is the clearest equity case. It contributes 10,455 records, of which 4,768 enter the primary analysis, and 420 receive a green energy pathway, giving an 18.49% modeled reduction. The composition is distinctive: 237 community solar or incentive candidates, 98 rooftop solar with financing, 83

Table 5. Base-scenario results by ZIP Code Tabulation Area

ZCTA	Rec.	Prim.	Green	Base	Res	Red	Aff
48120	1,554	608	236	136.2	74.4	45.40	0.29
48124	15,422	9,060	853	317.6	261.6	17.63	0.68
48126	10,455	4,768	420	350.4	285.6	18.49	0.42
48128	4,447	1,838	72	41.5	37.4	10.04	0.74
48228	31,309	6,171	310	185.3	156.3	15.66	0.29
All	**63,187**	**22,445**	**1,891**	**1,031.0**	**815.2**	**20.93**	**0.58**

Rec. is the number of GIS-validated records and Prim. the primary analysis population. Base and Res are modeled baseline and residual annual demand in GWh, Red the modeled percentage reduction, and Aff the median neighborhood affordability proxy of the residential buildings.

commercial or industrial candidates, 2 critical facility candidates, and no conventional higher-affordability rooftop recommendation.

The reason is evident in the socioeconomic data. Of its 4,441 residential primary buildings, 2,945 are affordability constrained and 1,496 are moderate, with none in the higher-affordability group, and the median affordability proxy is 0.416 against 0.735 in 48128. Technical screening alone would have identified 335 suitable residential buildings and implied conventional rooftop adoption for all of them. The equity-aware layer instead indicates that the same physical potential exists but requires a different delivery mechanism, which is a materially different planning conclusion.

4.6. Scenario-Based Sensitivity

Table 6 and Fig. 8(b) report the three scenarios. The modeled reduction ranges from 0.60% under conservative assumptions to 52.79% under optimistic assumptions, and the number of green pathway buildings ranges from 63 to 20,658. This spread is wide and constitutes the primary caveat on every absolute value reported in this paper.

The sensitivity is informative rather than merely cautionary. Under the conservative case a threshold of 0.70 exceeds the technical score of almost every residential building, so residential participation collapses to 25 buildings and the offset derives almost entirely from a few large nonresidential structures. The optimistic case shows the converse: at a threshold of 0.50 most of the residential stock qualifies, 5,486 buildings are routed to community solar, and the binding constraint shifts from technical suitability to program delivery capacity.

Two structural results are stable across the spread. The number of candidate substations receiving demand remains 36 in all three cases, and the number of low-utilization review candidates remains 12, 12, and 13. The reprioritization conclusion is therefore not an artifact of the base parameter choice, even though the magnitude of the demand reduction clearly is.

Table 6. Scenario assumptions and the resulting outcomes

Parameter	Cons.	Base	Optim.
Roof factor multiplier	0.85	1.00	1.15
EUI multiplier	1.10	1.00	0.90
Technical threshold	0.70	0.60	0.50
Affordability t_{low}	0.55	0.45	0.35
Affordability t_{high}	0.70	0.65	0.55
Solar offset multiplier	0.85	1.00	1.10
Community solar offset	0.20	0.30	0.45
Green pathway buildings	63	1,891	20,658
Baseline demand (TWh)	1.134	1.031	0.928
Residual demand (TWh)	1.127	0.815	0.438
Demand reduction (%)	0.60	20.93	52.79
Low-utilization candidates	12	12	13

All three scenarios use the same 22,445 primary analysis buildings and the same 36 candidate substations. Baseline demand differs between scenarios because the EUI multiplier is itself a scenario parameter.

The framework should accordingly be presented as a planning and scenario analysis tool rather than a forecast of adoption.

4.7. Limitations and Practical Interpretation

Five limitations bound the interpretation of these results. First, candidate substations are public map-derived locations and the building to substation association is spatial proximity rather than verified feeder connectivity, so Stage 2 outputs are screening priorities rather than network study conclusions. Second, building demand is modeled from floor area and an energy use intensity proxy rather than metered, and only 1.2% of residential records report an observed number of levels, so the demand match score is nearly constant within the residential stock.

Third, the solar resource is effectively uniform: all five ZCTAs receive an annual irradiance of 3.7834 kWh/m^2/day, because the study area is compact relative to the resolution of the climatological product. The sunlight term therefore acts as a regional feasibility factor rather than a building-specific variable, and no rooftop shading, tilt, or orientation analysis is performed. Fourth, the economic screen is weaker than it appears. Because irradiance, power density, performance ratio, installed cost, and electricity value are constants in the base scenario, the simple payback of (11) evaluates to 14.14 years for every building whose generation does not exceed its own demand, so the payback test excludes only three of the 276 technically suitable nonresidential buildings. The screen should be regarded as a scenario-level feasibility check and would become discriminating only with category-specific cost curves, incentive structures, or locational electricity prices.

Fifth, affordability is a neighborhood proxy and does not describe the household occupying a given building, and 26,714 generic or unclassified records were withheld from the energy model, so the reported totals are lower bounds on the potential of the full building stock. None of these limitations invalidates the comparative structure of the study, because the baseline and the proposed case are evaluated under identical assumptions and the same population, but each constrains the absolute values. The framework should be read as producing a prioritized, equity-aware shortlist for further engineering and program study rather than a deployment decision.

5. Conclusion

This paper presented a two-stage GIS framework linking building-level DER planning to grid location prioritization through a single explicit quantity, the residual demand. By decoupling technical suitability from deployment feasibility, neighborhood affordability selects the delivery mechanism of a green energy pathway rather than reducing the measured suitability of a building.

Applied to five census areas in southeastern Michigan using only public data, the framework produced a validated dataset of 63,187 buildings with 22,445 in the primary analysis and reduced modeled annual demand from 1.031 to 0.815 TWh. Two results are of general interest. Among technically suitable residential buildings, 55.2% were redirected toward community or financing-supported pathways, quantifying the gap between physical potential and realistic deployment mechanism. At the grid level, distributed adoption changed the rank of 24 of 36 candidate substations and the priority class of five while leaving the number of low-utilization locations unchanged, indicating that the effect of DERs on asset planning is a reordering of importance rather than a reduction of it. This result held across the full scenario range, whereas the magnitude of the demand reduction did not. Because candidate substations are identified through geographic proximity rather than verified feeder connectivity, these grid-level findings should be interpreted as a planning-level screening result rather than a confirmed network outcome.

Future work will incorporate utility feeder topology, metered interval demand, a higher-resolution irradiance product with shading analysis, improved attribution for the withheld records, and power flow verification of the reprioritized locations.

References

[1] P. S. Georgilakis and N. D. Hatziargyriou, A review of power distribution planning in the modern power systems era: Models, methods and future research, Electric Power Systems Research, vol. 121, pp. 89–100, Apr. 2015. https://doi.org/10.1016/j.epsr.2014.12.010

[2] T. N. Pham, R. Shah, M. N. Dao, N. Sultanova, and S. Islam, Low and medium voltage distribution network planning with distributed energy resources: A survey, IET Generation, Transmisson Distribution, vol. 17, no. 19, pp. 4711–4736, Oct. 2023. https://doi.org/10.1049/gtd2.12986

[3] J. L. Picard, I. Aguado, N. G. Cobos, V. Fuster-Roig, and A. Quijano-Lopez, Electric distribution system planning methodology considering distributed energy resources: A contribution towards real smart grid deployment, Energies, vol. 14, no. 7, pp. 1924, Mar. 2021. https://doi.org/10.3390/en14071924

[4] P. Gagnon, R. Margolis, J. Melius, C. Phillips, and R. Elmore, Rooftop solar photovoltaic technical potential in the United States: A detailed assessment, National Renewable Energy Laboratory, Golden, CO, USA Jan. 2016.

[5] J. A. Jakubiec and C. F. Reinhart, A method for predicting city-wide electricity gains from photovoltaic panels based on LiDAR and GIS data combined with hourly Daysim simulations, Solar Energy, vol. 93, pp. 127–143, Jul. 2013. https://doi.org/10.1016/j.solener.2013.03.022

[6] D. Palmer, E. Koumpli, I. Cole, R. Gottschalg, and T. Betts, A GIS-based method for identification of wide area rooftop suitability for minimum size PV systems using LiDAR data and photogrammetry, Energies, vol. 11, no. 12, pp. 3506, Dec. 2018. https://doi.org/10.3390/en11123506

[7] F. Biljecki, Y. S. Chow, and K. Lee, Quality of crowdsourced geospatial building information: A global assessment of OpenStreetMap attributes, Building and Environment, vol. 237, pp. 110295, 2023. https://doi.org/10.1016/j.buildenv.2023.110295

[8] K. Jenkins, D. McCauley, R. Heffron, H. Stephan, and R. Rehner, Energy justice: A conceptual review, Energy Research and Social Science, vol. 11, pp. 174–182, Jun. 2016. https://doi.org/10.1016/j.erss.2015.10.004

[9] E. O'Shaughnessy, G. Barbose, R. Wiser, and S. Forrester, Income-targeted marketing as a supply-side barrier to low-income solar adoption, iScience, vol. 24, no. 10, pp. 103137, Oct. 2021. https://doi.org/10.1016/j.isci.2021.103137

[10] D. A. Sunter, S. Castellanos, and D. M. Kammen, Disparities in rooftop photovoltaics deployment in the United States by race and ethnicity, Nature Sustainability, vol. 2, no. 1, pp. 71–76, Jan. 2019. https://doi.org/10.1038/s41893-018-0204-z

[11] A. Aznar and D. Gagne, Low-income community solar: Utility return considerations for electric cooperatives, National Renewable Energy Laboratory, Golden, CO, USA 2018.

[12] N. Mohandes, A. Sanfilippo, and M. Al Fakhri, Modeling residential adoption of solar energy in the Arabian Gulf region, Renewable Energy, vol. 153, pp. 842–854, Jun. 2020.
https://doi.org/10.1016/j.renene.2020.02.042

[13] OpenStreetMap contributors, Copyright and license, 2026.
[Online] URL: https://www.openstreetmap.org/copyright Accessed on: Aug. 72026

[14] U.S. Census Bureau, TIGER/Line shapefiles, 2025.
[Online] URL: https://www.census.gov/geographies/mapping-files/time-series/geo/tiger-line-file.html Accessed on: Aug. 72026

[15] U.S. Census Bureau, American Community Survey 5-year data (2020–2024), 2025.
[Online] URL: https://www.census.gov/data/developers/data-sets/acs-5year.html Accessed on: Aug. 72026

[16] NASA POWER Project, POWER application programming interface data access documentation, 2025.
[Online] URL: https://power.larc.nasa.gov/docs/services/api/ Accessed on: Aug. 72026

[17] U.S. Energy Information Administration, 2018 Commercial Buildings Energy Consumption Survey: Consumption and expenditures highlights, 2022.
[Online] URL: https://www.eia.gov/consumption/commercial/ Accessed on: Aug. 72026

[18] U.S. Energy Information Administration, 2020 Residential Energy Consumption Survey: Consumption and expenditures, 2023.
[Online] URL: https://www.eia.gov/consumption/residential/ Accessed on: Aug. 72026

[19] National Renewable Energy Laboratory, PVWatts calculator technical reference, 2025.
[Online] URL: https://developer.nrel.gov/docs/solar/pvwatts/ Accessed on: Aug. 72026

[20] I. Ramos-Diez, S. Barilari, J. Ljunggren, S. Hellsten, and N. Ferreras-Alonso, A Python GIS-based multi-criteria assessment to identify suitable areas for photovoltaic energy measures, ISPRS International Journal of Geo-Information, vol. 15, no. 4, pp. 157, Apr. 2026.
https://doi.org/10.3390/ijgi15040157

[21] U.S. Department of Housing and Urban Development, CPD income and rent limits, 2025.
[Online] URL: https://www.hudexchange.info/programs/home/home-income-limits/ Accessed on: Sept. 42026

[22] V. Ramasamy, J. Zuboy, E. O'Shaughnessy, D. Feldman, J. Desai, M. Woodhouse, P. Basore, and R. Margolis, U.S. solar photovoltaic system and energy storage cost benchmarks, with minimum sustainable price analysis: Q1 2022, National Renewable Energy Laboratory, Golden, CO, USA 2022.